Experimental two-way communication with one photon

Francesco Massa[1*], Amir Moqanaki[1], Flavio Del Santo[1], Borivoje Dakic[1,2], Philip Walther[1*]

[1]*Vienna Center for Quantum Science and Technology (VCQ),*
Faculty of Physics, University of Vienna,
Boltzmanngasse 5, Vienna A-1090, Austria
[2]*Institute for Quantum Optics & Quantum Information (IQOQI),*
Austrian Academy of Sciences,
Boltzmanngasse 3, Vienna A-1090, Austria

To whom correspondence should be addressed;
E-mail: francesco.massa@univie.ac.at (F.M.); philip.walther@univie.ac.at (P.W.)
(Dated: February 16, 2018)

Superposition of two or more states is one of the fundamental concepts of quantum mechanics and provides the basis for several advantages quantum information processing offers. In this work, we experimentally demonstrate that quantum superposition permits two-way communication between two distant parties that can exchange only one particle once, an impossible task in classical physics. This is achieved by preparing a single photon in a coherent superposition of the two parties' locations. Furthermore, we show that this concept allows the parties to perform secure quantum communication, where the transmitted bits and even the direction of communication remain private. These important features can lead to the development of new quantum communication schemes, which are simultaneously secure and resource-efficient.

In the last decades, quantum information science has led to insights that promise to revolutionize the future of information processing technologies. Among them, quantum communication, the ability of transmitting a quantum state between a sender and a receiver, is one of the earliest known applications [1]. The main motivation behind the efforts in this direction is that quantum systems allow communication features that are not achievable with classical objects, like, for example, security against eavesdropping, as shown for quantum key distribution (QKD)[2–5] or quantum secure direct communication [6–8]. In terms of efficiency, it was shown, both theoretically and experimentally, that quantum protocols lead to reductions in the amount of information to be transmitted to perform a specific task, which can also be exponential, compared to the classical ones [9–12]. At the same time, there is great interest in schemes that allow to optimize the amount of physical resources to be used for communication, like in the case of quantum dense coding [13–15] and quantum random access codes [16–18].

On this line, a recent theoretical study [19] shows that, by means of quantum superposition, it is possible to achieve two-way communication between two distant parties which only exchange a single particle once. This is impossible in classical physics, where two-way communication can be realized only if the parties exchange two particles, one per party, or if the same particle goes back and forth between them. Thus, for this specific task, quantum mechanics allows a reduction in number of particles to be used or, alternatively, in the time employed for the communication. We implement the protocol proposed in [19] with single photons and demonstrate the two-way signalling between the communication parties. From a fundamental point of view, the present work shows interesting analogies to recent research in quantum causality [20–24], of which some concepts have also been experimentally demonstrated [25, 26].

We further analyse the protocol and show that it grants secure direct communication between the two parties, given that they actually share a single-particle superposition state. Interestingly, even the direction of communication can be hidden, a feature that connects our work to the field of anonymous quantum communication, where either the sender or the receiver of a message (or both) are supposed to be hidden [27–29]. To approach real-life situations, we devise a version of the protocol that is robust against losses and randomness in photon emission. Our results, therefore, highlight several aspects of quantum superposition and can pave the way for novel secure and resource-efficient quantum communication schemes.

DEMONSTRATION OF TWO-WAY SIGNALLING WITH A SINGLE PHOTON

In order to show two-way signalling, we consider a communication game in which a referee respectively assigns two random input bits, x and y, to two distant communication parties, named Alice and Bob, who are then allowed to exchange one particle. We call τ the time it takes for the exchange to be completed, that is the interval between the time at which the particle leaves Alice's or Bob's location and the time at which it is detected. We assume τ shorter than the time required to a physical object to travel more than once the distance between Alice and Bob (see figure 1). When the exchange is completed, the referee asks Alice and Bob to reveal two output bits, a and b: they win the game if they both guess correctly the value of the other player's input (i.e. if $a = y$ and $b = x$). This game can be considered a variation of the well known "guess your neighbour's input" (GYNI) game [30]. Under the constraint that the parties can only exchange one particle within the time window τ, only two possible causal relations between variables x, y, a and b, are possible: either x influences a and b, whereas y influences b only (corresponding to a one-way communication from Alice to Bob) or y influences a and b, whereas x influences a only (one-way communication from Bob to Alice). Accordingly, the joint probability distribution $p(ab|xy)$ results in a classical mixture of the two one-way signalling distributions. This imposes to the probability of winning the game a maximal value of 1/2 [31].
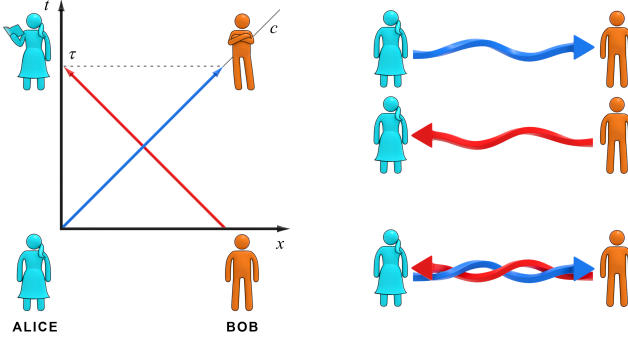
Let us now consider the case of a single quantum parti-

Figure 1 Diagrams of communication between two distant parties. Classically, a single carrier travelling with finite speed, bounded by the speed of light c, can transmit information either from Alice to Bob (blue arrow) or from Bob to Alice (red arrow) only, if the time τ allowed for the communication is shorter than the time the carrier takes to travel more than once the distance between Alice and Bob (space-time diagram on the left). An information carrier in quantum superposition permits to overcome this limitation and carry out a two-way communication process (scheme on the right).

cle prepared in a coherent superposition between Alice's and Bob's respective locations:

$$|\psi_{in}\rangle = \frac{1}{\sqrt{2}}(\widehat{a}^\dagger + \widehat{b}^\dagger)|0\rangle, \qquad (1)$$

where $\widehat{a}^\dagger$ and $\widehat{b}^\dagger$ are the particle creation operators at Alice's and Bob's location, respectively, and $|0\rangle$ is the vacuum state. Alice and Bob encode the bits x and y in the phase of the particle, obtaining the state:

$$|\psi_{encode}\rangle = \frac{1}{\sqrt{2}}((-1)^x\,\widehat{a}^\dagger + (-1)^y\,\widehat{b}^\dagger)|0\rangle. \qquad (2)$$

In the middle of the path between Alice and Bob a beam splitter is placed. This is a device that can either reflect or transmit the particle with 50% probability, with the two possibilities being in a coherent superposition. The action of the beam splitter can be expressed by the following transformations:

$$\widehat{a}^\dagger \longrightarrow \frac{1}{\sqrt{2}}(\widehat{a}^\dagger + \widehat{b}^\dagger), \qquad (3)$$

$$\widehat{b}^\dagger \longrightarrow \frac{1}{\sqrt{2}}(\widehat{a}^\dagger - \widehat{b}^\dagger). \qquad (4)$$

Due to interference, after the device, the final state of the photon is:

$$|\psi_{fin}\rangle = \begin{cases} \widehat{a}^\dagger|0\rangle, & \text{if } x=0 \text{ and } y=0, \\ \widehat{b}^\dagger|0\rangle, & \text{if } x=0 \text{ and } y=1, \\ -\widehat{b}^\dagger|0\rangle, & \text{if } x=1 \text{ and } y=0, \\ -\widehat{a}^\dagger|0\rangle, & \text{if } x=1 \text{ and } y=1. \end{cases} \qquad (5)$$

This means that, by checking whether they detect the particle or not, Alice and Bob can infer the parity of x and y. This piece of information, combined to the knowledge of their input bits, allows them to ideally win the game with probability 1, thus showing genuine two-way communication.
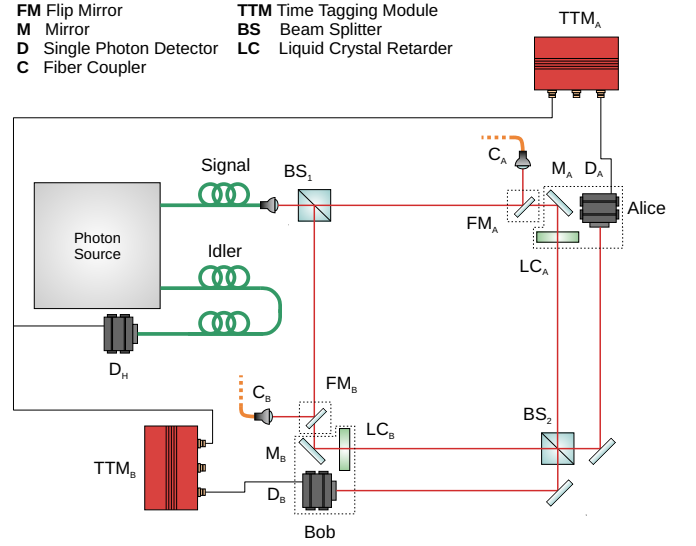

Figure 2 Experimental set-up. Single-photon pairs are produced through spontaneous parametric down-conversion (SPDC). For each pair, one photon is used to herald the presence of the other one, which is sent to a Mach-Zehnder interferometer. Alice and Bob occupy the area around the mirrors M_A and M_B, where, for each of them, a liquid-crystal phase shifter, for phase encoding, and a photon detector are placed. After the second beam splitter, the photons can travel to Alice or Bob, according to the parity of the input bits. Removable mirrors are used to measure the time at which Alice and Bob receive the photons from the source for the purposes explained in the main text. They steer light to fibers that can be connected to either Alice's or Bob's detector. For more details about the set-up, we refer to the appendix.

The set-up for the implementation of the game is shown in figure 2. A heralded single photon is sent to one of the input ports of a first beam splitter, which puts the photon in a superposition state between Alice's and Bob's locations. Then, Alice and Bob encode their bits in the phase of the photon and direct it to a second beam splitter, which creates the final state $|\psi_{fin}\rangle$. This scheme represents a Mach-Zehnder interferometer.

In order to prove that each photon cannot be exchanged more than once between the two parties, we measure the delay between two events: the reception of the photon before the encoding and the final detection after the second beam splitter. Actually there are four delays to be measured, according to whether the initial reception and the final detection of the photon are considered at Alice or Bob. The delays are slightly different due to the fact that the implemented interferometer is rectangular. The results of these measurements are shown in table I. It can be seen that, in all the cases, the time τ necessary for the photon exchange to be completed is shorter than the time the photon would take to travel twice the minimum distance between Alice and Bob (reference time) by more than 3 standard deviations. This excludes the possibility that the photon travels back and forth between Alice and Bob with less than 1% risk. More details about the adopted measurement method and the data analysis can be found in the appendix.

We estimate the probability of winning the game by using a random sequence of 100 input bit pairs, one every 0.5 s. In this time interval, we register an average number of photon detections of about 15×10^3. For each setting, therefore, we compute the probability of success by counting how

Initial Reception	Final Detection	Delay (ns)
Alice	Alice	7.1 ± 0.4
Alice	Bob	8.2 ± 0.4
Bob	Alice	7.5 ± 0.3
Bob	Bob	8.5 ± 0.4
Reference time: (10.1 ± 0.1) ns		

Table I Time measurement results. The four possible delays between the initial reception and the final detection of the photon at Alice or Bob are shown in the table. They are compared to the time the photon would take to travel the minimum distance between the two parties, roughly equal to the diagonal of the interferometer, at the speed of light in vacuum (reference value). For each delay, the measurements were taken by unblocking only the corresponding path and recording the arrival-time statistical distributions for reception and final detection, respectively. The uncertainty on each interval is obtained from the standard deviations of the associated arrival-time distributions, dominated by the time jitter of our detectors. The uncertainty on the reference value is not statistical and comes from the uncertainty on the measurement of the minimum distance between Alice and Bob.
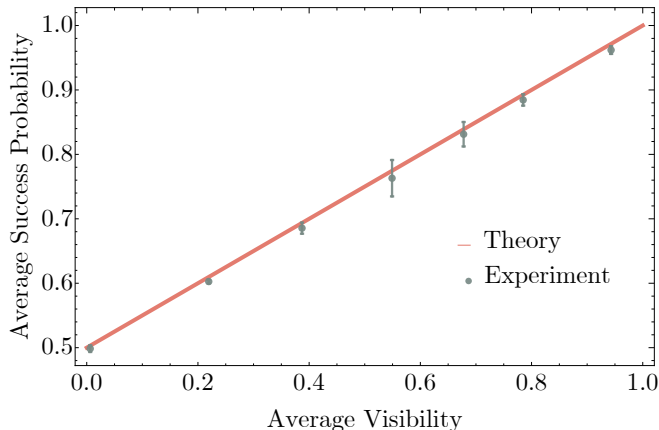

Figure 3 Success probability vs interferometric visibility. The plot shows the behaviour of the probability of winning the game with respect to the quality of the single-photon interference produced by the state Alice and Bob share, which is quantified by the average interferometric visibility. The visibility is varied by delaying one interferometric path with respect to the other: at zero visibility the two photon wave packets travelling in the two arms no longer overlap at the final beam splitter and the interference is completely cancelled. The equation of the red theoretical curve is $y = 0.5(x + 1)$. The error on each probability is the standard error on the mean, obtained from the statistical variation over the sequence of input bits. For each point in the plot, a different random input sequence of bit pairs is generated.

many photons go to the "right" output and then averaging the probability over the input sequence. Figure 3 shows the measured success probability for different values of the interferometric visibility in our Mach-Zehnder, averaged over the two output ports. The visibility at each port is defined as $(N_{MAX} - N_{MIN})/(N_{MAX} + N_{MIN})$, where N_{MAX} and N_{MIN} are the maximum and minimum number of detections at that port. The success probability surpasses the classical limit as soon as the visibility is greater than zero. For our maximally achieved visibility of 0.941 ± 0.007, we observe the maximal success probability of 0.961 ± 0.006. At zero visibility the success probability is 0.498 ± 0.006, comparable with the maximum achievable value in the classical case (0.5). At this point, the effect of the quantum superposition is totally nullified.

In order to claim we have effectively implemented a two-way communication protocol with a single particle, we also need to demonstrate that Alice and Bob cannot share two or more photons at the same time. This can be shown by measuring the heralded second-order correlation function at zero delay of our photon-pair source, $g^{(2)}(0)$ [32]. This is a number between 0 and 1, quantifying the amount of multi-photon emission from the source. A value of $g^{(2)}(0)$ closer to 1 would imply that two or more photons are sent simultaneously to the interferometer. For an ideal heralded single-photon source this number is 0. We measure $g^{(2)}(0) = 0.004 \pm 0.010$, which is statistically compatible to 0 and in line with the lowest values obtained in quantum optics experiment [33]. For more details about how this value was obtained we refer to the corresponding section of the appendix.

BIT ENCRYPTION AND HIDDEN DIRECTION OF COMMUNICATION

The implemented scheme can also be used by the parties to simultaneously transmit any two bits x and y with one particle only. Interestingly the values of the bits are encrypted. This can be easily seen by re-writing equation 2 in another form:

$$|\psi_{encode}\rangle = \frac{1}{\sqrt{2}}(-1)^x \, (\widehat{a}^\dagger + (-1)^{x \oplus y} \, \widehat{b}^\dagger)|0\rangle, \quad (6)$$

where the symbol $\oplus$ stands for modulo-2 sum of the bits. The only piece of information that is extractable from the state $|\psi_{encode}\rangle$ is the relative phase $(-1)^{x \oplus y}$. This means that a potential eavesdropper, Eve, does not have direct access to the transmitted bits but only to the parity, p ($p = x \oplus y$), therefore she could guess them with a probability of 50% at best.

If, by repeating the procedure several times, one of the two parties transmits a one-time pad, a truly random sequence that can be used only once, the message transmitted by the other one is then fully secure against eavesdropping [34], once it is assumed that they actually share the state $|\psi_{encode}\rangle$ for each pair of transmitted bits. Furthermore Eve cannot know which party is transmitting the one-time pad and which one the message, meaning that the direction of communication is hidden.

A rigorous implementation of the described communication protocol would require a deterministic single-photon source, providing one photon for each pair of bits Alice and Bob want to transmit. However, truly deterministic sources still represent an experimental challenge. Furthermore, losses in communication links would render any deterministic photon emitter a probabilistic source. Therefore, in order to simulate real-life situations, we devise and experimentally demonstrate a version of the protocol that can be realized with a probabilistic source. We set a communication interval for each pair of bits x and y, which in our case is 0.5 s, and reduce the emission rate of our source so as to have an average number of detections per communication interval of about 3. Here we consider the sum of the detections Alice and Bob record. If Alice (Bob) receives one or more photons during a given communication interval, she(he) infers that $x \oplus y = 0$ (= 1), and $x \oplus y = 1$ (= 0) otherwise. The fact that, on average, more than one photon is transmitted for a bit pair does not affect the security of the protocol, since the information Eve can extract from each particle is always the same and not enough for her to determine the value of the bits. An error occurs every time in a given interval at least one photon goes to the "wrong"
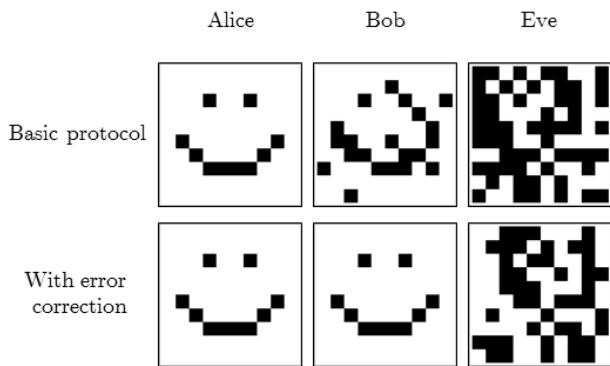
Figure 4 Example of secure communication. An example in which Alice sends a message in the form of a figure and Bob a random sequence with the same length is presented. The three columns report, in the order, the figure sent by Alice, that one received by Bob and the parity of the bits sent by Alice and Bob, the only piece of information Eve can get from the superposition state. Two cases are shown: the basic protocol, where each bit pair is sent once with an average probability of success of 75% and the error-corrected protocol, where each bit pair is sent 5 times, with an average probability of success of 99%.

output or when no photon is detected by both Alice and Bob at the end of the interval. These errors can be minimized by suitably choosing the average number of detections per interval (see appendix for more details). Error correction protocols can also be applied to increase the success probability. We provide an example by implementing simple schemes where each bit pair is sent 3 and 5 times, respectively, and the most frequent outcome for each pair of bits is chosen. The average success probability of the communication protocol, measured by counting the successful transmission events, for different random sets of 100 bit pairs is 0.75 ± 0.02. By implementing the error correction schemes with 3 and 5 repetitions per bit pair, we obtain success probabilities of 0.89 ± 0.02 and 0.99 ± 0.02, respectively. We report an example where Alice sends a 10 pixels $\times$ 10 pixels image in black and white, corresponding to 100 bits, and Bob sends a sequence of 100 random bits. Figure 4 shows the outcome of the communication both for the basic protocol and for the error-corrected one with 5 repetitions per bit pair.

In conclusion, we have shown experimentally that, by using quantum superposition, it is possible to perform two-way communication between two parties that exchange only a single photon once. We have ruled out the possibility that the photon travels back and forth between them or that two or more photons are simultaneously used. Furthermore, we have designed and implemented a protocol for two-way communication between the parties that exploits a probabilistic single-photon source and shown that, under certain assumptions, it allows secure direct communication between them, with the additional feature of hidden communication direction. Our insights set an important basis for the realization of new communication protocols to be used for real-world applications.

[1] Bennett, C. H., Brassard, G. in *Int. Conf. Computers, Systems and Signal Processing, Bangalore*, 175-179 (1984).

[2] Ekert, A. K., Quantum cryptography based on bell theorem. *Phys. Rev. Lett.* **67,** 661 (1991).

[3] Bennett, C. H., Quantum cryptography using any two nonorthogonal states. *Phys. Rev. Lett.* **68,** 3121 (1992).

[4] Ursin, R. et al., Entanglement-based quantum communication over 144 km. *Nat. Phys.* **3,** 481 (2007).

[5] Wang, S. et al., Experimental demonstration of a quantum key distribution without signal disturbance monitoring. *Nat. Photonics* **9,** 832 (2015).

[6] Long, G.-L. et al., Quantum secure direct communication and deterministic secure quantum communication. *Front. Phys., 2,* 251-272(2007).

[7] Hu, J.-Y. et al., Experimental quantum secure direct communication with single photons. *Light Sci. App.* **5,** e16144 (2016).

[8] Zhang, W. et al., Quantum secure direct communication with quantum memory. *Phys. Rev. Lett.* **118,** 220501 (2017).

[9] Massar, S., Quantum fingerprinting with a single particle. *Phys. Rev. A* **71,** 012310 (2005).

[10] Trojek, P. et al., Experimental quantum communication complexity. *Phys. Rev. A* **72,** 050305 (2005).

[11] Xu, F. et al., Experimental quantum fingerprinting with weak coherent pulses. *Nat. Commun.***6,** 8735 (2015).

[12] Guan, J.-Y. et al., Observation of quantum fingerprinting beating the classical limit. *Phys. Rev. Lett.* **116,** 240502 (2016).

[13] Bennett, C. H., Wiesner, S. J., Communication via one- and two-particle operators on Einstein-Podolsky-Rosen states. *Phys. Rev. Lett.* **69,** 2881-2884 (1992)

[14] Mattle, K., Weinfurter, H., Kwiat, P. G., Zeilinger, A., Dense coding in experimental quantum communication. *Phys. Rev. Lett.* **76,** 4656-4659 (1996)

[15] Barreiro, J. T., Wei, T.-C., Kwiat, P. G., Beating the channel capacity limit for linear photonic superdense coding. *Nat. Phys.* **4,** 282-286 (2008)

[16] Ambainis, A., Leung, D., Mancinska, L., Ozols, M., Quantum random access codes with shared randomness. Preprint at https://arxiv.org/abs/0810.2937(2009)

[17] Pawłowski, M., Żukowski, M., Entanglement-assisted random access codes. *Phys. Rev. A* **81,** 042326 (2010)

[18] Tavakoli, A., Hameedi, A., Marques, B., Bourennane, M., Quantum random access codes using single d-level systems, *Phys. Rev. Lett.* **114,** 170502 (2015)

[19] Del Santo, F., Dakić, B., Two-way communication with a single quantum particle. *Phys. Rev. Lett.* **120,** 060503 (2018).

[20] Feix, A., Araújo, M., Brukner, Č., Quantum superposition of the order of parties as a communication resource. *Phys. Rev. A* **92,** 052326 (2015).

[21] Guérin, P. A., Feix, A., Araújo, M., Brukner, Č. Exponential communication complexity advantage from quantum superposition of the direction of communication. *Phys. Rev. Lett.* **117,** 100502 (2016).

[22] Oreshkov, O., Costa, F., Brukner, Č., Quantum correlations with no causal order. *Nat. Commun.* **3,** 1092 (2012).

[23] Chiribella, G., D'Ariano, G. M., Perinotti, P., Quantum circuit architecture. *Phys. Rev. Lett.* **101,** 060401 (2008).

[24] Chiribella, G., D'Ariano, G. M., Perinotti, P., Valiron, B., Quantum computations without definite causal structure. *Phys. Rev. A* **88,** 022318 (2013).

[25] Procopio L. M. et al., Experimental superposition of orders of quantum gates. *Nat. Commun.* **6,** 7913 (2015).

[26] Rubino, G. et al., Experimental verification of an indefinite causal order. *Sci. Adv.* **3,** e1602589 (2017).

[27] Christandl, M., Wehner, S. in *Int. Conf. Theory and Application of Cryptology and Information Security, Chennai,* 217-235 (2005).

[28] Brassard, G., Broadbent, A., Fitzsimons, J., Gambs, S., Tapp, A., Anonymous quantum communication. *Int. Conf. Theory and Application of Cryptology and Information Security, Kuching,* 460-473 (2007).

[29] Sun, S., Waks, E., Secure quantum routing. Preprint at https://arxiv.org/abs/1607.03163 (2016).

[30] Almeida, M. L. et al., Guess your neighbor's input: a multipartite nonlocal game with no quantum advantage. *Phys. Rev. Lett.* **104,** 230404 (2010).

[31] Branciard, C., Araújo, M., Feix, A., Costa, F., Brukner, Č., The simplest causal inequalities and their violation. *New J. Phys.* **18,** 013008 (2015).

[32] L. Mandel, E. Wolf, *Optical Coherence and Quantum Optics*(Cambridge Univ. Press, Cambridge, 1995).

[33] Eisaman, M., Fan, J., Migdall, A., Polyakov, S., Single photon sources and detectors. *Rev. Sci. Instr.,* **82,** 071101 (2011).

[34] C. Shannon, Communication theory of secrecy systems. *Bell Syst. Techn. J.,* **28,** 656-715(1949).

[35] Kim, T., Fiorentino, M., Wong, F. N. C., Phase-stable source of polarization-entangled photons using a polarization Sagnac interferometer. *Phys. Rev. A,* **73,** 012316 (2006).

[36] Malitson, I. H., Interspecimen comparison of the refractive index of fused silica. *J. Opt. Soc. Am.* **55,** 1205-1209 (1965)

[37] Jin, R.-J. et al., Efficient detection of an ultra-bright single-photon source using superconducting nanowire single-photon detectors, *Opt. Comm.* **336,** 47-54 (2015)

APPENDIX

The single-photon source

We use an SPDC-based single-photon source in a Sagnac configuration [35], with a 20-mm-long periodically-poled potassium tytanyl phosphate (PPKTP) crystal. The Sagnac loop was realized using a dual-wavelength polarizing beam splitter and two mirrors. The crystal converts a photon at 395 nm into two photons at 790 nm and orthogonal polarizations. The produced photons were coupled into single-mode fibers: one of them was sent to the Mach-Zehnder interferometer and the other was directly sent to a silicon avalanche photo-diode (APD) for heralding the presence of its twin in the interferometer. The use of polarizers for both photons of each pair ensure that a defined polarization state is produced, in particular $|H\rangle|V\rangle$, where H stands for "horizontal" and V for "vertical").

The interferometric set-up

The interferometer we built is depicted in figure 2 in the main text. The distance between the mirror M_A and the beam splitter BS_2 is (106 ± 1) cm, whereas the distance between M_B and BS_2 is (119 ± 1) cm. The minimum distance between the regions occupied by Alice and Bob is the distance between the sides of the liquid-crystal phase shifters, equal to (156 ± 1) cm. The geometry of the interferometer is chosen so as to maximize the difference between the time photons take to travel from mirrors M_A and M_B to the detectors and the time they would take to travel twice the minimum distance between Alice and Bob, given the limits of space on our optical table. The two flip mirrors FM_A and FM_B are placed at 10.0 cm of distance from M_A and M_B, respectively. They are used to steer light to two fiber couplers, C_A and C_B, connected to two 2-m-long multi-mode fibers. The coupling in the multi-mode fibers is about 96%. The distance between the flip mirrors and the couplers is also 10.0 cm, so that photons reach the fibers at the same time they would arrive at M_A and M_B if FM_A and FM_B were not there. The uncertainty on all these distances was estimated to be 0.5 cm. The detectors D_A and D_B are silicon APDs. We use them in a free-space configuration for the final detection of the photons but we connect them to the fibers from the couplers for the acquisition of the photon arrival-time distributions at the mirrors M_A and M_B. All the arrival times are measured by means of two different time-tag logic units, one for each detector, and they are always referred to the detection of the heralding photon, used as a trigger.

The interferometer is passively stabilized by thermal and vibrational isolation so that the phase between the two arms is stable for about one minute. After this time, the phase can be re-set by means of a piezo actuator mounted in a trombone delay line, which can be used to delay one arm with respect to the other and therefore to change the interference visibility. We re-set the piezo every 50 input bit pairs, corresponding to about 25 s. There are still some residual fluctuations of the phase around the stability point in this time interval, which, together with the standard poissonian fluctuations in the number of counts, determine the errors on the success probabilities reported in the main text.

The polarization of the photons entering the interferometer is set to "horizontal" (H), that means parallel to the optical table, by means of two waveplates and a polarizer, placed before BS_1. The slow axes of the two liquid-crystal phase shifters are aligned to the photon polarization. The refractive index along these axes depends on the voltage applied to the liquid crystal. We characterize the phase-shift with respect to the voltage and set a phase-shift of 0 to encode the bit 0" and of π to encode the bit 1".

Analysis of the photon arrival-time distributions

Let us call Δt_{AB} the time photons take to travel from the mirror M_A to the detector D_B along the arms of the interferometer. In the same way we call Δt_{AA}, Δt_{BA}, Δt_{BB} the time photons take to go from M_A to D_A, from M_B to D_A and from M_B to D_B, respectively. The procedure we adopted to measure Δt_{AB} is the following:

1. we block all the possible paths for the photons except for that one going from M_A to D_B.

2. For each photon pair, we register the delay between the detection of the heralding photon and the detection of its correlated photon at D_B, after it travels through the interferometer. In this way we acquire the arrival-time distribution for the final detection at D_B, referred to the herald detection.

3. We turn up the flip mirror FM_A and connect the multimode fiber from the coupler C_A to the detector D_B. After correcting for the delay introduced by the fiber, we acquire the arrival-time distribution at M_A, as in point 2.

4. We fit the two obtained distributions with gaussian functions and, for each of them, we consider the mean value and the standard deviation.

5. We calculate Δt_{AB} as the difference of the mean values of the two distributions. Since the detections take place at the same detector and we use the same time-tag unit, the difference is not affected by further electronic delays. The error on Δt_{AB} is the sum in quadrature of the standard deviations of the two distributions.

For the measurement of Δt_{AA}, Δt_{BA} and Δt_{BB}, we follow analogous procedures. In order to correct the delays introduced by the fibers, their length is measured with a fibermeter. We obtain (2.080 ± 0.004) m and (2.088 ± 0.004) m for the fibers connected to C_A and C_B, respectively. The refractive index of the core, made of pure silica, is taken from [36]. The errors on the fiber lengths and on the refractive index are negligible with respect to the standard deviation of the arrival time distributions. Figure A1 shows the acquired arrival-time distributions, together with the related gaussian fits.

In the plots, two secondary peaks for each main peak can be noticed, which are probably due to optical reflections in the set-up. The total number of counts in the secondary peaks is approximately 5% of that in the corresponding main peak. However, in the implementation of the game and the communication protocol, for the coincidence counting between

the final detection of the photon in the interferometer and the heralding photon, we set a coincidence window of 1 ns around the delays obtained from the fits of the final arrival-time distributions: in this way the coincidences that are related to the secondary peaks are not considered.

It can be observed that the arrival-time distributions at D_A and D_B are slightly asymmetric with respect to the peak. We hypothesize that this is due to the fact that the photons, in the free-space-detection case, hit the edge of the active area of the APD, thus producing some capacitive effect in the resulting electric signal.

For the detection we use single-photon counting modules from Excelitas, model SPCM-AQRH. This model has a typical jitter time (standard deviation) of 0.149 ns. Since each peak is obtained by coincidence detection between two modules, if we consider only the effect of the jitter, we expect a standard deviation of 0.210 ns. This value is compatible with those obtained for fiber-coupled detection but significantly lower than those obtained in case of free-space detection. We again ascribe the mismatch to the imperfect alignment of the beam in the case of free-space detection.

As it can be seen from table I, the quantity $|\Delta t_X - \Delta t_{ref}|/\sigma_X$ is always above 3, where Δt_{comp} is the reference value and X can be AA, AB, BA or BB, respectively. This allows us to claim with less than 1% of risk that the two values are not compatible and then that the time the photons take to go from the mirror M_A or M_B to the detector is shorter than the time they would take to travel twice the minimum distance between Alice and Bob. In this procedure of comparison we neglected the error on Δt_{comp} because the corresponding relative error is more than 4 times lower than that on any Δt_X.

Measurement of the second-order correlation function at zero delay

In order to measure the heralded second-order correlation function at zero delay, $g^{(2)}(0)$, we steer the photons to the couplers C_A and C_B, by means of the flip mirrors FM_A and FM_B, and we connect the related fibers to the detectors D_A and D_B. We consider the two-fold coincidence rates between the detection of the heralding photon and the detection of its correlated photon at D_A or D_B, which we call respectively CC_{HA} and CC_{HB}, and the three-fold coincidence rate, CC_{HAB}. We set the delays between the detections electronically in order to maximize CC_{HA} and CC_{HB} and in these conditions we evaluate $g^{(2)}(0)$, according to the following formula([37]):

$$g^{(2)}(0) = \frac{2 \times C_H \times CC_{HAB}}{(CC_{HA} + CC_{HB})^2},$$

where C_H is the rate of single counts for the heralding photons.

We average the rates over 3 minutes and obtain $g^{(2)}(0) = 0.004 \pm 0.01$, where the error is calculated from poissonian uncertainty on the count rates. This value is measured for 7 mW of pump power in the source.

Error correction

Our scheme can also be implemented for non-ideal photon sources. In case of a probabilistic source, such as photon sources based on SPDC, we modify the scheme as follows:

1. Alice and Bob decide a communication interval, during which a pair of bits should be transmitted. At the end of the communication interval, they register the received bit.

2. For each communication interval, the source emits on average N photons, m of which are detected by Alice or Bob.

3. If Alice (Bob) receives 1 or more photons during the communication interval, she (he) assumes that the parity of the transmitted bits is 0 (1). From the parity she (he) recovers the value of the bit Bob (Alice) has sent. If Alice (Bob) receives no photons by the end of the communication interval, she (he) assumes that the parity of the transmitted bits is 1 (0).

4. Alice and Bob repeat the procedure until the end of the message they want to transmit.

The only difference between this protocol and the basic protocol is that there is the possibility Alice and Bob receive more than one photon per communication interval. There are two possible sources of errors: 1) one of more photons is detected at the wrong output or 2) no photon is detected at all. Therefore the probability of error for each communication interval is $p_{err} = p_0 + p_{wrong}$, where p_{wrong} is the probability of case 1 and p_0 of case 2.

We assume that the number of photons Alice and Bob globally detect follows a poissonian distribution with m as mean value. The probability that n photons are detected is therefore:

$$p(n) = e^{-m}\frac{m^n}{n!}.$$

From the previous equation, it is straightforward that $p_0 = e^{-m}$. Given that n photons are detected, the probability that at least one out of them is detected at the wrong output is $1 - p_s^n$, where p_s is the probability of success of the original protocol, that is the probability that a photon is detected at the right output. By keeping this in mind we get:

$$p_{err} = e^{-m} + \sum_{n=1}^{\infty} p(n)(1 - p_s^n)$$
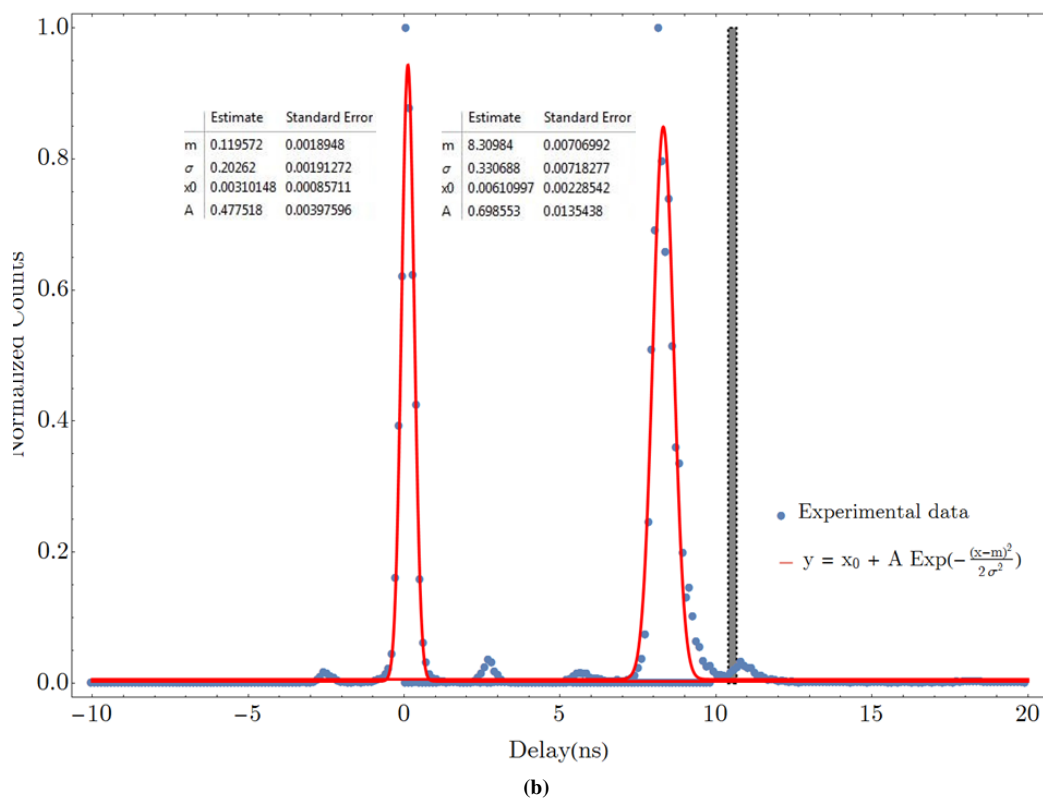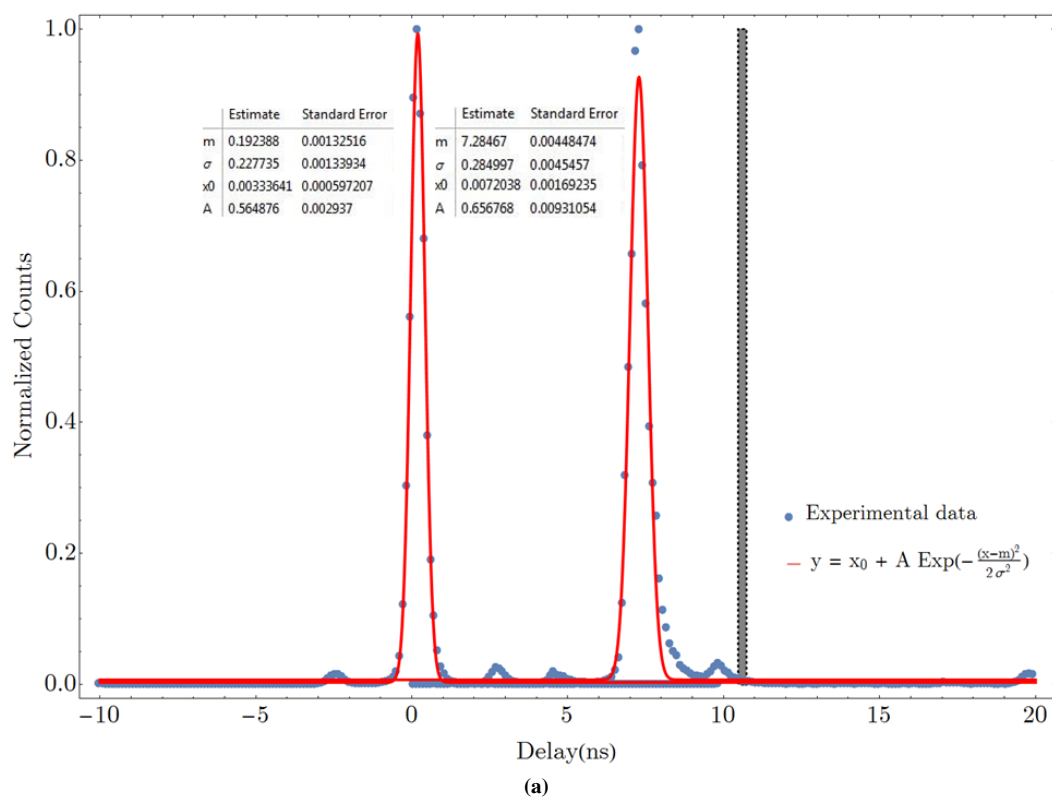$$= e^{-m}(1 + \sum_{n=1}^{\infty} \frac{m^n(1 - p_s^n)}{n!}).$$

For low values of m, p_0 tends to 1, while, as $m \to \infty$, the second term, p_{wrong} tends to 1, thus dominating the sum. This means that between these two extremes there must be a value of m, that we call m_{opt}, for which p_{err} is minimum. This value depends of course on p_s, in particular it increases if p_s increases, reflecting the fact that one can use more photons if for each photon the probability of success is higher.

Since the values of p_s for our set-up are around 0.95, we calculate that m_{opt} is around 3. We reduce the pump power of our source until we obtain globally about 3 detections per communication interval. We measure a success probability

of the protocol over 10 sets of 100 random pairs of bits of 0.75 ± 0.02. The error is calculated by considering the standard deviation of the probability over the sets and by dividing it by the square root of the number of sets, thus obtaining an error on the average value. The average number of detections, m and the probability of success per photon, p_s, over the sets are respectively 3.34 ± 0.06 and 0.935 ± 0.008. By inserting these values in our poissonian model, we calculate a success probability of 0.77 ± 0.02, perfectly compatible with the measured value. We note that, considering $p_s = 0.935$, the maximum theoretical success probability is 0.772, for $m = 2.919$.

As mentioned in the main text, we implement an error correction scheme, based on the repetition of the same bit pair 3 and 5 times, respectively. In both cases we average over 4 sets of 100 bit pairs, for a total of 1200 and 2000 transmitted bit pairs, respectively. In the case of 3 repetitions, we obtain a success probability of 0.89 ± 0.02. The expected value in this case is 0.90 ± 0.01, considering that $m = 2.62 \pm 0.05$ and $p_s = 0.948 \pm 0.006$. For the case of 5 repetitions, the measured success probability results to be 0.99 ± 0.02 while the expected value is 0.97 ± 0.01, with $m = 3.736 \pm 0.004$ and $p_s = 0.960 \pm 0.004$. All the measured values are perfectly compatible with the expected ones, thus confirming the validity of the poissonian model we assume.
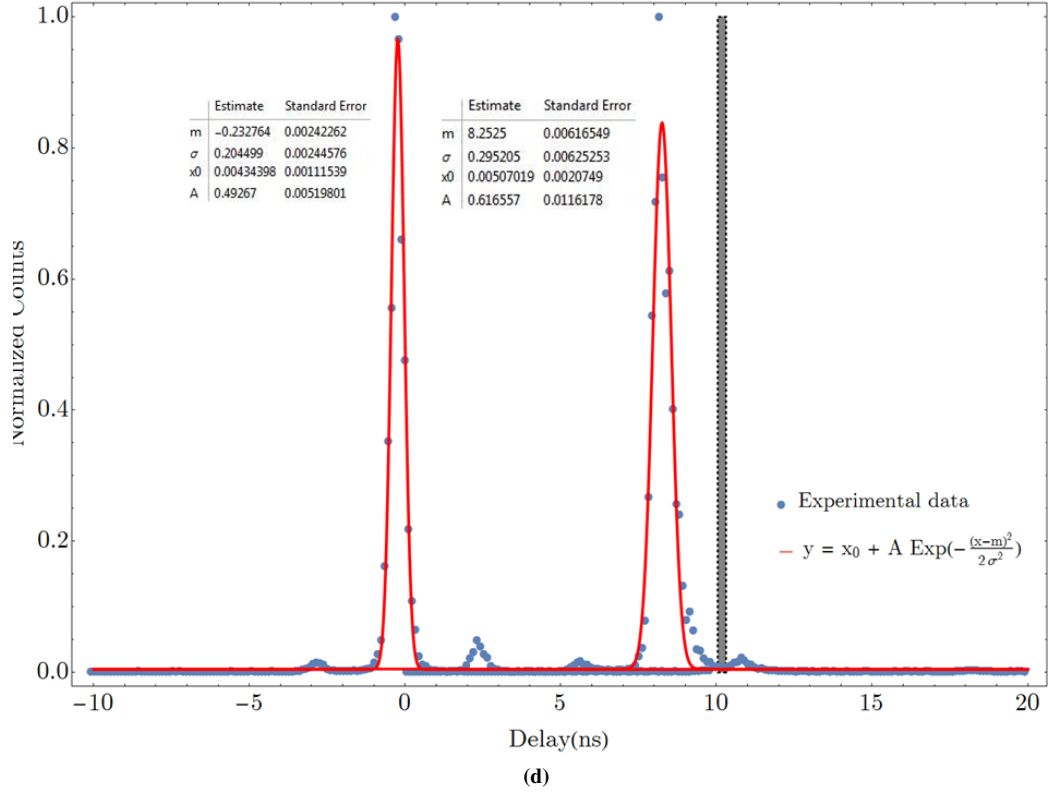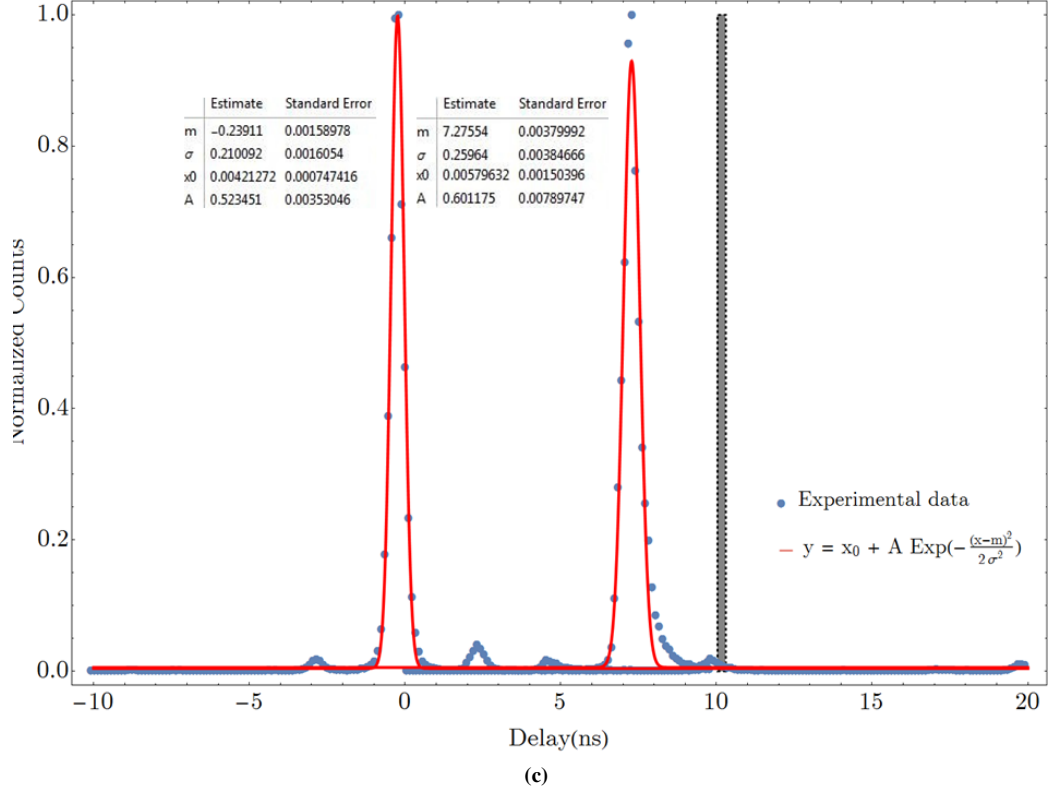
(a)

(b)

(c)

	Estimate	Standard Error		Estimate	Standard Error
m	−0.23911	0.00158978	m	7.27554	0.00379992
σ	0.210092	0.0016054	σ	0.25964	0.00384666
$x0$	0.00421272	0.000747416	$x0$	0.00579632	0.00150396
A	0.523451	0.00353046	A	0.601175	0.00789747

- Experimental data
- $y = x_0 + A\,\mathrm{Exp}\!\left(-\frac{(x-m)^2}{2\sigma^2}\right)$

(d)

	Estimate	Standard Error		Estimate	Standard Error
m	−0.232764	0.00242262	m	8.2525	0.00616549
σ	0.204499	0.00244576	σ	0.295205	0.00625253
$x0$	0.00434398	0.00111539	$x0$	0.00507019	0.0020749
A	0.49267	0.00519801	A	0.616557	0.0116178

- Experimental data
- $y = x_0 + A\,\mathrm{Exp}\!\left(-\frac{(x-m)^2}{2\sigma^2}\right)$

Figure A1. Arrival-time distributions. The figures are related to the four possible time intervals Δt_{AA} (a), Δt_{AB} (b), Δt_{BA} (c) and Δt_{BB} (d). The arrival times at M_A or M_B, after correcting for the fiber delay (peaks on the left), and those one at the final detectors D_A or D_B (peaks on the right) are reported on the x-axis. These times are expressed as delays with respect to the heralding photon detection. The two peaks in each figure are fitted with the gaussian function in the plot boxes (red curves). The parameters of the fits are shown to the left of the corresponding peak. The black vertical bars indicate the time window, including the error, at which the photons would arrive at D_A or D_B if they travelled twice the minimum distance between Alice and Bob.